A Platinum Open Access Journal for Organic Chemistry

Paper

Free to Authors and Readers | DOAJ Seal | *Arkivoc* **2021**, part iv, 51-64

Migrastatin analogues with an (*E*)-alkene at the ring C-3: synthesis, conformational analysis and biological evaluation

Sinclair Sweeney,[a] Patrick McArdle,[a] Bartłomiej Taciak,[b] Stefania Robakiewicz,[b] Magdalena Król,[b] and Paul V. Murphy[a]*

[a] *School of Chemistry, National University of Ireland Galway, University Road, Galway, Ireland H91 TK33*
[b] *Department of Cancer Biology, Institute of Biology, Warsaw University of Life Sciences, Warsaw, Poland*
Email: paul.v.murphy@nuigalway.ie

Dedicated to Professor Dr. Horst Kunz on the occasion of his 80th birthday

Received 06-05-2020 **Accepted** 07-08-2020 **Published on line** 08-07-2020

Abstract

Synthesis of one acyclic and four macrocyclic analogues of migrastatin with an *E*-alkene at C-3 is described. The route involves ring-closing metathesis, which gave *ca.* 1:1 mixtures of stereoisomeric alkenes. The crystal structure for a macrolactam with an *E*-alkene at C-3 and *Z*-alkene at C-8 was obtained with a brief study of macrocycle conformation by molecular mechanics and coupling constant analysis. Amide rotamers are also observed by NMR spectroscopy. Preliminary *in vitro* biological study indicates that the new compounds may have limited potential as inhibitors of tumor cell migration.

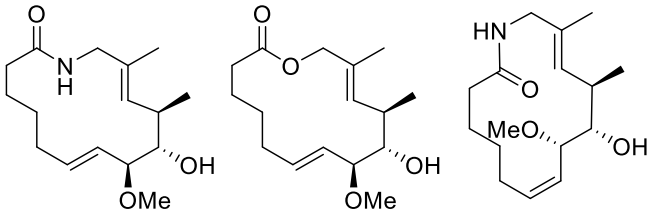

New macrocyclic compounds synthesised as analogues of migrastatin

Keywords: Migrastatin, analogue synthesis, macrocycles, macrolactams, conformation

1. Introduction

Migrastatin **1** (Scheme 1), is a polyketide[1-3] containing a 14-membered macrocyclic lactone, which has been reported to inhibit tumor cell migration. Structurally less complex analogues or truncated[4] analogues of migrastatin such as **2-5**, have shown improved inhibition of tumour cell migration than migrastatin, *in vitro*[5]. Moreover, macroketone **3** and macrolactam **4** inhibited the migration of highly metastatic tumour cells in mouse models *in vivo*.[6-7] Our group have been involved in the synthesis of migrastatin and its analogues[8] and through collaboration with Anderson and Nobis have reported that macroketone **3** inhibited E-cadherin dynamics *in vivo*, in a manner consistent with increased cell adhesion and reduced invasive potential.[9] The synthesis of metastasis inhibitors continues as an area of interest for research.[10-20]

The macrocyclic ring of migrastatin has an alkene with *Z* configuration at its C-3, and there are *E*-alkenes at C-8 and C-12. We report here the synthesis of five analogues of the core of migrastatin **6-10**, including macrolactams and macrolactones with an *E*-alkene at C-3. Lactam analogues of the migrastatin macrolactone were found previously to be more stable in vivo and thus considered important for this reason. In addition to the synthesis we provide information on the conformation of one macrolactam, including its crystal structure. We also report preliminary data on abilities of compounds to inhibit migration of cancer cells.

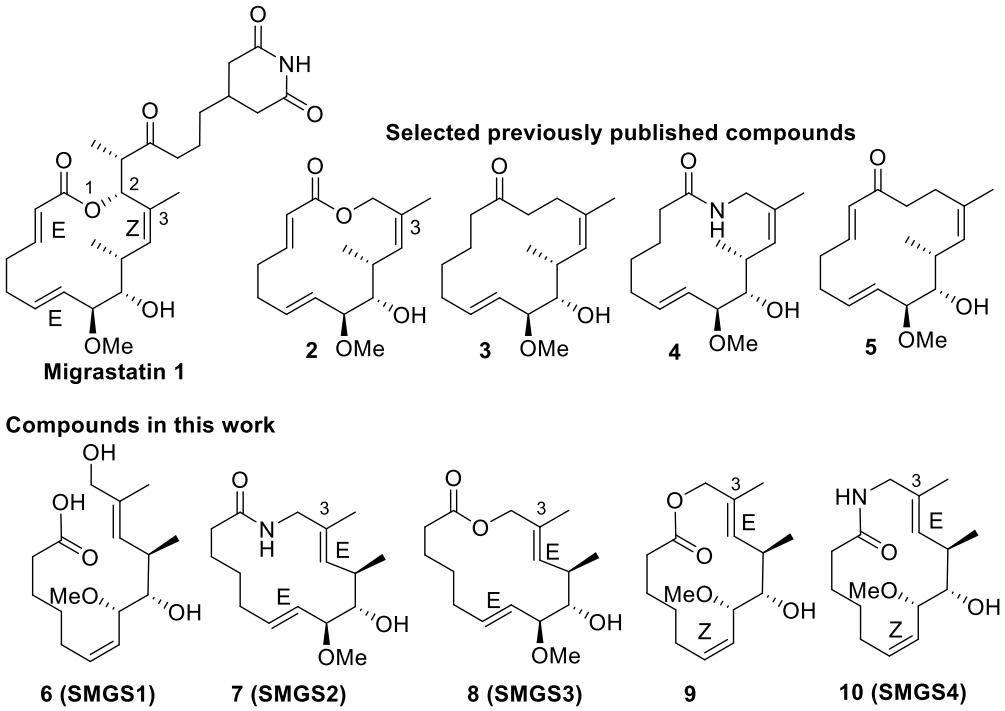

Scheme 1: Structures of compounds **1-10.**

2. Results and Discussion

2.1 Syntheses of macrocyclic compounds

Syntheses of migrastatin analogues use ring closing metathesis (RCM)[21] for macrocyclisation. Thus, dienes needed for the preparation of macrocyclic rings with *E*-alkenes at C-3 were first prepared from known ester **11** (Scheme 2).[22] The subsequent steps we used were similar to those used by Danishefsky and co-workers in

synthesis of **2-4**. Thus, the reduction of **11** with DIBAL-H gave the allylic alcohol **12**[5] (Scheme 2). The reaction of **12** with diphenylphosporyl azide in the presence of DBU followed by the Staudinger reaction gave an amine intermediate, which after coupling with 6-heptenoic acid in the presence of EDC gave **14**, whereas direct Mitsunobu reaction of **12** with 6-heptenoic acid gave ester **13**. Heating of ester **13**, which has the *E*-configuration at C-3, with the Grubbs-II catalyst in toluene at reflux for 45 minutes gave a mixture of cyclic alkenes (8E:8Z = 50:50, 46% isolated yield). Repeating this reaction over a longer time (90 minutes) gave rise to a modest increase amount of the *E*-alkene (56:43 with 42% yield). The Grubbs-II catalyst promoted reaction of amide **14** gave also a mixture of alkenes (8Z:8E = 1.2:1, 46%), with the *Z*-isomer preferred. Removal of the TBS protecting groups with HF-pyridine, from the intermediates obtained, gave **7-10**. The stereoselectivities observed in the RCM reactions differ to those where there was a Z-alkene at C-3; preparations of **2-5** by RCM gave only *E*-isomers. Macrocycle **9** was subjected to saponification to give acyclic compound **6**. Acyclic compounds were shown to inhibit tumour cell migratory capacity in previous work.

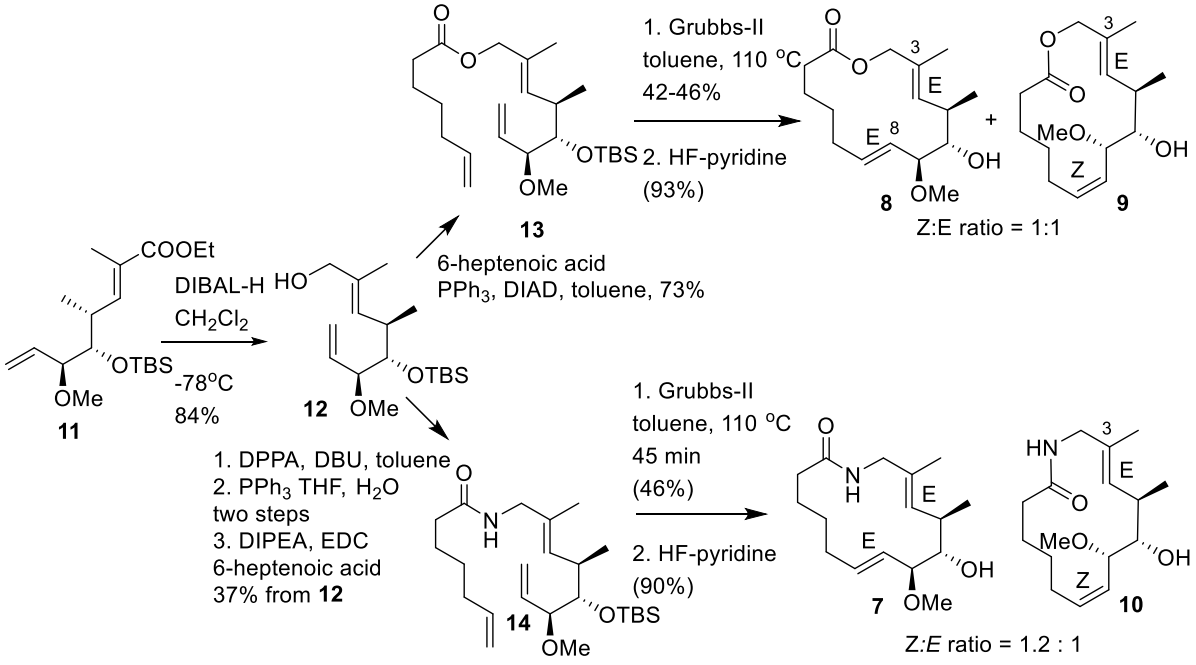

Scheme 2. Synthesis of **7-10.**

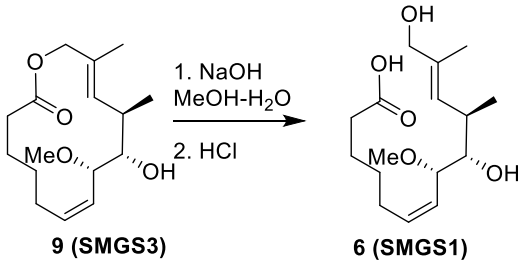

Scheme 3 Synthesis of **6.**

2.2 Conformation of macrolactam 10

In the case of lactam **10**, crystals suitable for X-ray diffraction were obtained from EtOAc and the crystal structure was therefore determined (Figure 1). There were two crystallographically distinct molecules in the

asymmetric unit and both had the same conformation. The *E*-configuration at C-3 as well as the Z-configuration at C-8 and the presence of *trans*-amide was confirmed for **10** in the solid state. The dihedral angles as found in the crystal structure for the NH to C-10 backbone of the macrocycle are given in Table 1. Vicinal coupling constants (^3J values, Table 1) were also extracted from the ^{1}H-NMR spectrum of **10** recorded at 500 MHz ($CDCl_3$) and these are listed also in Table 1. The MestReJ[23] programme uses a range of different equations for the computation of vicinal coupling constants (*J* values) in ^{1}H-NMR spectra. This relates to the original work of Karplus who defined a relationship between the *J* value and dihedral angle.[24-25] In Table 1, the calculated *J* values from Barfield-Smith[26-27] and Karplus equations as implemented by MestReJ are shown and they generally compare well with those obtained by recording the ^{1}H-NMR spectrum in $CDCl_3$ for **10**, with the largest discrepancy between calculated and measured ^3J values being 2.4 Hz for the coupling between the NH and one of the C-2 protons when using the Barfield-Smith equation and which was 1.8 Hz for use of the Karplus equation. Aside from the dihedral angle, the *J* value can be influenced by factors such as electronegative substituents and the position of those same electronegative substituents, which may contribute to differences between calculated and observed *J* values. The data indicates that the backbone from the amide to C-10 of the macrocycle in the crystal structure and in $CDCl_3$ are similar. The X-ray crystal structure was also compared with the lowest energy structure generated after a conformational search, generating, minimising and evaluation energies of 10,000 conformers using Macromodel[28] (Schrodinger Inc., LLC, New York, USA) with implementation of the OPLS-AA force field.[29] The two structures were superimposed (Figure 2a) and there was good correlation (RMSD = 0.25) between the lowest energy structure obtained by this conformational search with that of the X-ray crystal structure for the C-2 to C-10 backbone atoms. Five conformers were found for the lactam within 10 kJ/mol of the global minimum and these were superimposed and shown in Figure 2b. During the conformer search, the interconversion between the *trans* and *cis* amide was enabled and two of the low energy conformers were found to be the *cis*- rather than the *trans*-amide. Preliminary viewing of the ^{1}H-NMR spectrum for **10** gave the impression of impurities being present. However closer examination indicated there are two signal sets in the spectrum of **10** which can be attributed to the observation of both the *cis*-amide and *trans*-amide of the lactam; these stereoisomers are interconverting (chemical exchange) and the rate of interconversion enables NMR spectroscopy observe them.[30-34] The ratio was determined to be 9:1 by integration of NMR signals with the *trans*-amide assumed to be favoured, as supported by the trend in stability (*trans* amide more stable than *cis* amide) predicted using Macromodel. The signal at δ 5.39 (triplet) is assigned to the C-8 alkene proton for the lactam with the *trans* configured amide, whereas the triplet at δ 5.60 is assigned to the C-8 alkene proton of the lactam with the *cis*-amide. There is evidence for interconversion between these amide rotamers, as provided by both 1D-NOE and 2D-NOE experiments. The basis for using 1D-NOE or 2D-NOE is that cross-peaks or correlations can be observed that are opposite in phase (negative NOEs) to the normal NOE enhancements (positive NOEs), because they arise through chemical exchange. Irradiation of the signal at δ 5.39 using a 1D-NOE experiment led to indirect irradiation of the signal at δ 5.60 through saturation transfer, indicating the nuclei interconvert. A negative NOE cross-peak, between these two signals is also apparent in the 2D-NOE spectrum of **10**. Other negative crosspeak correlations are observed in the 2D spectrum, including one between the signal for H-2b at δ 3.54 (dd) of the major rotamer and with the signal at δ 3.74 ppm (dd), the latter assigned to H-2b of minor rotamer.

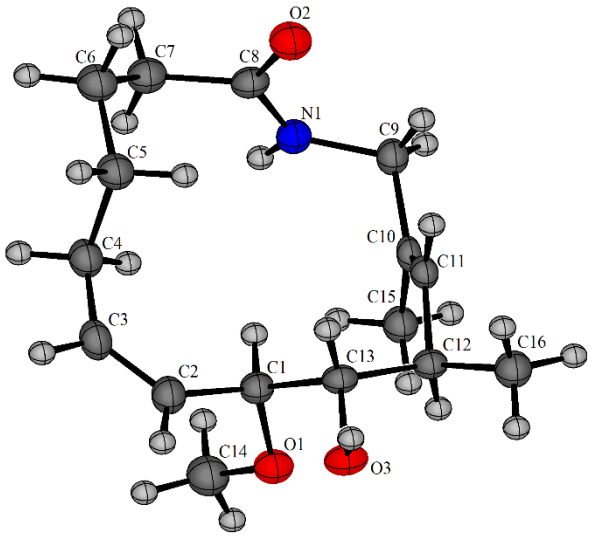

Figure 1. X-Ray crystal structural diagram for **10**. The numbering used here does not correspond with IUPAC nomenclature numbering. C2-C3 labelling here corresponds to the *Z*-alkene.

Table 1. Dihedral angles and coupling constants (*J*) of compound **10 (SMGS4)**

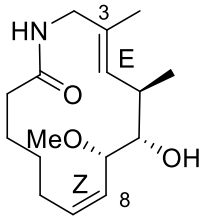

10

Atoms defining dihedral angle	Angle from crystal structure	Calculated J (Hz, Barfield-Smith)	Calculated J (Hz, Karplus)	Observed J (Hz, $CDCl_3$)	Angle in lowest energy structure (Macromodel OPLSAA)
H-N-C2-H2a	162.4	10.1	9.5	7.7	157.4
H-N-C-H2b	52.2	5.1	3.6	5.3	41.0
H4-C4-C5-H5	164.6	10.4	9.7	10.1	161.4
H5-C5-C6-H6	171.1	11.0	10.1	10.0	177.8
H6-C6-C7-H7	62.9	3.2	2.5	3.5	79.5
H7-C7-C8-H8	178.1	11.1	10.3	10.1	177.3
H9-C9-C10-H10a	36.2	8.0	5.6	6	51.3
H9-C9-C10-H10b	154.6	9.2	8.7	10.3	166.7

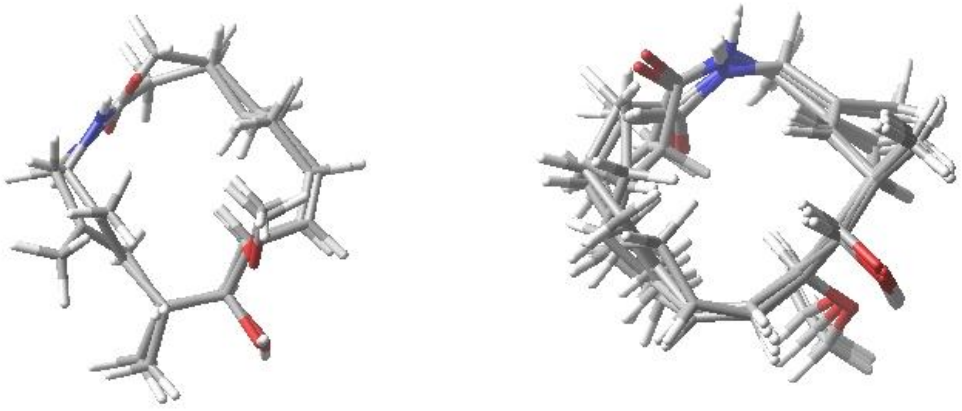

(a) (b)

Figure 2. (a) Overlap of X-ray structure with lowest energy structure generated by conformational search in Macromodel is shown on the left. Overlay was generated by superimposing macrocyclic backbone atoms NH to C-10 (RMSD = 0.25) (b) Five superimposed isomers generated within 10 kJ/mol of global minimum as obtained from conformational search using Macromodel are shown on the right. Two of these five stereoisomers had a *cis*-amide conformation; the lowest energy conformer had the *trans*-amide.

2.3 Evaluation of compounds as tumor cell migration inhibitors

Firstly, cell viability assays showed compounds were generally not toxic to cells (see Supp. Info.). Then four compounds **6-8** and **10 (SMGS1-4)**, were selected for the wound healing assay which was performed using different human cancer cell lines (pancreatic: MiaPaCa2, and breast: MDA-MB231, MDA-MB361 and MCF7) and all four compounds reduced wound closure for MiaPaCa2 cells after 24h compared to the control (Figure 3). The macrocyclic compounds **SMGS2-4** reduced wound closure for MDA-MB361 cells but no significant inhibition of wound closure was observed for MDA-MB231 or MCF7 cells. None of **6-8** and **10**, nor macrolactam **4** inhibited migration of these cancer cell types using the transwell migration assay (Boyden chamber assay). The Boyden chamber assay is considered a more comprehensive measure of inhibitory capacity towards cell migration. The wound repair study was also carried out for macrolactone **8** and known migration inhibitor **4** using the lung tumour A549 cell line. The wound repair assay showed cell inhibition over 24 h for macrolactam **4** with much less inhibition for **8**. The transwell migration assay showed that **4** has the highest % inhibition of the A549 cell migration, but that **8** had low inhibition.

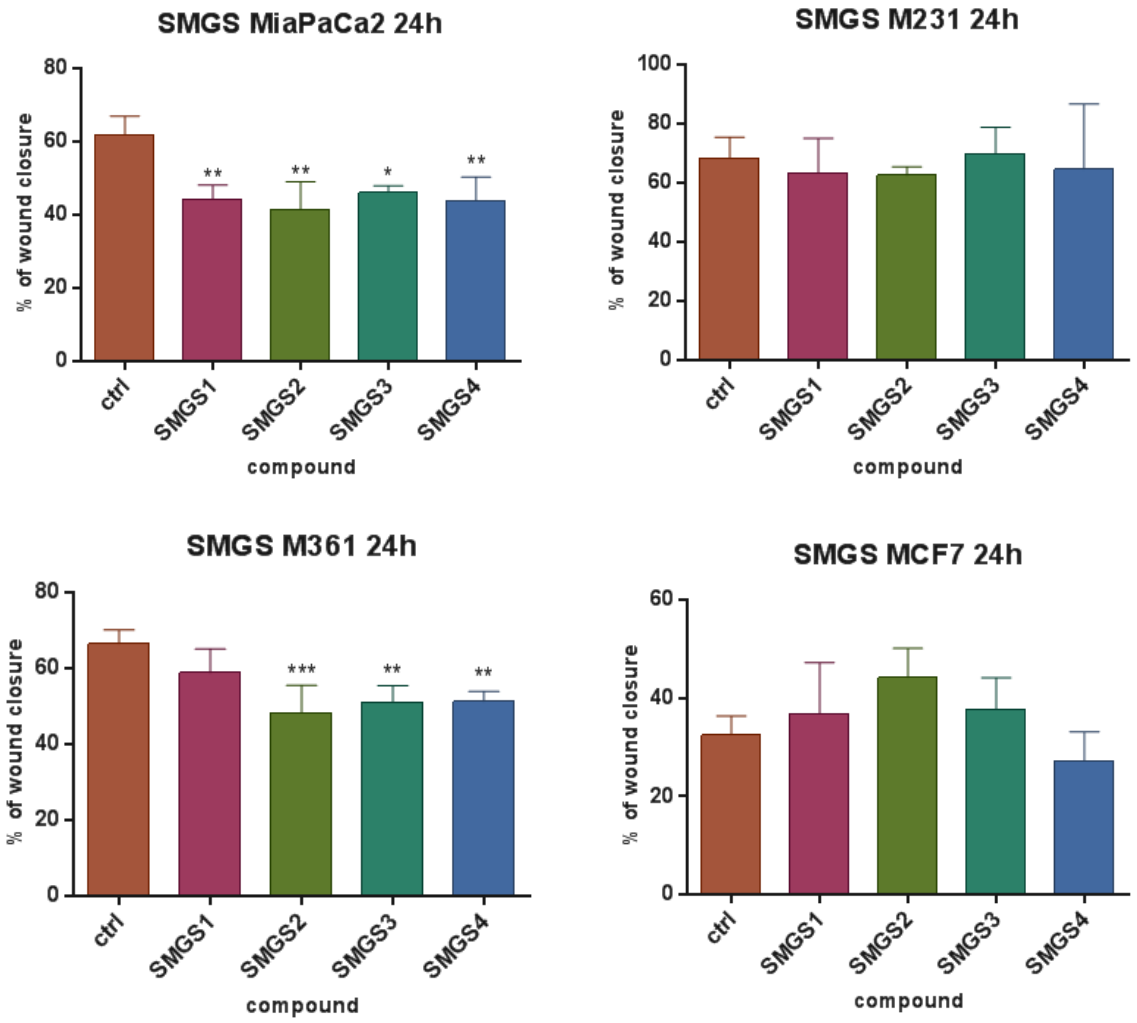

Figure 3. Bar graphs show the effect of the migrastatin analogues on migration of various cell lines after 24 h of incubation. Compounds significantly retarded the process of wound healing in MiaPaCa2 cells and three compounds retarded the process for MDA-MB361 cells (M361 on graphs). No significant retardation compared to control was observed for MCF7 and MDA-MB231 cells (M231 on graphs). Results with $p < 0.001$, and $p < 0.01$ were considered to be highly relevant and denoted ** and ***. Results with $p < 0.05$ were determined to be relevant and are indicated with *.

Conclusions

Herein the synthesis of analogues of migrastatin, where there is an *E*-alkene present at C-3, is described, providing compounds for study as potential anti-metastatic agents. Ring closure metathesis reactions showed an increased preference for the *Z*- or *cis* alkene in such analogues compared to compounds with the *Z*-alkene at C-3. The crystal structure of a macrolactam, and analysis of coupling constants in ^{1}H-NMR spectra, as well as conformational searching techniques in Macromodel provided information on the conformation of the macrocyclic ring. The presence of amide rotamers in a macrolactam derivative was supported by 1D and 2D ^{1}H-NMR experiments. The preliminary biological studies indicate the new analogues may have limited potential as tumour cell migration inhibitors.

Experimental Section

General. ^{1}H-NMR spectra were recorded at 500 MHz and ^{13}C spectra at 126 MHz. The chemical shifts are reported in parts per million (ppm). The coupling constants are reported in Hertz (Hz) and the resonance patterns are reported from ^{1}H-NMR spectra with notations as the following: br (broad), s (singlet), d (double), t (triplet), q (quartet) and m (multiplet). ^{1}H-NMR signals were assigned with the aid of gCOSY. ^{13}C signals were assigned with the aid of DEPT-135, gHSQCAD and gHMBCAD. IR spectra were recorded using thin film on NaCl or germanium plates. Optical rotations were determined at the sodium D line at 23 ^{o}C. TLC was performed on aluminium sheets pre-coated with Silica Gel 60 (HF254, E. Merck) and spots visualized by UV and charring with 1:20 H_2SO_4-EtOH or with 1:1 $KMnO_4$ (1% w/v solution)-$NaHCO_3$ (5% w/v solution) or with cerium molybdate stain. Flash chromatography was generally employed and was carried out using Silica Gel 60 (0.040-0.630 mm, E. Merck) and employed a stepwise solvent polarity gradient correlated with the TLC mobility. Chromatography solvents used were EtOAc, dichloromethane (Riedel-deHaen), cyclohexane, pentane and MeOH (Sigma Aldrich). Anhyd. DMF and anhydrous toluene were used as purchased from Sigma-Aldrich. Solvents THF, dichloromethane and methanol were used as obtained from a Pure-Solv^{TM} solvent purification system.

(4R,5S,6S,E)-5-(tert-Butyldimethylsilyloxy)-6-methoxy-2,4-dimethylocta-2,7-dien-1-ol (12).[5] To ester **11** (*E:Z* = 44:1, 625 mg, 1.75 mmol), in dichloromethane (90 mL), DIBAL-H (6.2 mL, 6.20 mmol, 1.0 M solution in hexane) was added at -78 °C and the resulting solution was stirred at -78 °C for 2 h. The mixture was quenched with satd aq potassium sodium tartrate (50 mL), diluted with dichloromethane (50 mL) and was then vigorously stirred at room temperature for 3 h. The aq layer was extracted with dichloromethane (4 × 50 mL), the combined organic layers were dried and the solvent was then removed *in vacuo*. Chromatography (petroleum ether-EtOAc 10:1) gave **12** (469 mg, 84%) as a colourless oil; ^{1}H NMR (500 MHz, chloroform-d) δ 5.65 (ddd, *J* 17.5, 10.4, 8.1 Hz, 1H), 5.43 (d, *J* 9.3 Hz, 1H), 5.30 - 5.23 (overlapped signals, 2H), 3.98 (overlapped signals, 2H), 3.49 (dd, *J* 7.0, 3.3 Hz, 1H), 3.40 (t, *J* 7.5 Hz, 1H), 3.21 (s, 3H, OMe), 2.56 (m, 1H), 1.64 (s, 3H), 0.93-0.88 (overlapped signals, 12H, 4 x CH_3), 0.06 (s, 3H, SiCH_3), 0.02 (s, 3H, SiCH_3); ^{13}C NMR (126 MHz, chloroform-d) δ 135.5 (CH), 133.2 (C), 131.2 (CH), 118.7 (CH_2), 86.4 (CH), 78.1 (CH), 69.3 (CH_2), 56.3 (OCH_3), 34.3 (CH), 26.3 (C(CH_3)$_3$), 18.7 (C(CH_3)$_3$), 14.1 (CH_3), 13.9 (CH_3), -3.6 (SiCH_3), -4.6 (SiCH_3).

(4*S*,5*S*,6*S*,*E*)-5-(*tert*-Butyldimethylsilyloxy)-6-methoxy-2,4-dimethylocta-2,7-dienylhept-6-enoate (13). To alcohol **12** (150 mg, 0.48 mmol) in anhydrous toluene (15 mL) was added 6-heptenoic acid (130 µL, 0.96 mmol) and triphenylphosphine (352 mg, 1.34 mmol) while stirring. Diisopropyl azodicarboxylate (264 µL, 1.34 mmol) was added dropwise to the solution and the mixture was stirred for 3 h. The mixture was then quenched with satd aq NH_4Cl (30 mL) and the aq phase was extracted with EtOAc (3 x 20 mL). The combined organic layers were then dried over Na_2SO_4 and the solvent was removed. Flash chromatography (petroleum ether-EtOAc, 50:1) gave **13** as a yellow oil (149 mg, 73%); ^{1}H NMR (500 MHz, chloroform-d): δ 5.79 (ddt, *J* 17.0, 10.2, 6.7 Hz, 1H), 5.64 (ddd, *J* 17.2, 10.4, 8.1 Hz, 1H), 5.48 (dq, *J* 9.4, 1.3 Hz, 1H), 5.32 – 5.22 (overlapped signals, 2H), 5.03 – 4.93 (overlapped signals, 2H), 4.44 (2 x AB d, 2H), 3.49 (dd, *J* 7.0, 3.1, 1H), 3.39 (t, *J* 7.9 Hz, 1H), 3.21 (s, 3H), 2.56 (m, 1H), 2.32 (overlapped signals, 2H), 2.09 – 2.04 (overlapped signals, 2H), 1.68–1.63 (overlapped signals, 2H), 1.61 (d, *J* 1.4 Hz, 3H), 1.46 – 1.39 (overlapped signals, 2H), 0.92 (d, *J* 6.7 Hz, 3H), 0.90 (s, 9H), 0.06 (s, 3H), 0.01 (s, 3H); ^{13}C NMR (126 MHz, $CDCl_3$) δ 173.7 (C), 138.6 (CH), 135.4 (CH), 134.1 (CH), 128.6 (C), 118.7 (CH_2), 114.8 (CH_2), 86.4 (CH), 78.0 (CH), 70.1 (CH_2), 56.3 (CH_3), 34.4 (CH), 34.3 (CH_2), 33.5 (CH_2), 28.5 (CH_2), 26.3 (CH_3), 24.6 (CH_2), 18.7 (C), 14.2 (CH_3), 13.8 (CH_3), -3.6 (CH_3), -4.6 (CH_3); HRMS-ESI: calcd for $C_{24}H_{44}O_4NaSi$: 447.2907; Found 447.2902.

(7*E*,9*S*,10*S*,11*R*,12*E*)-10-Hydroxy-9-methoxy-11,13-dimethyloxacyclotetradeca-7,12-dien-2-one (8) and (7*Z*,9*S*,10*S*,11*R*,12*E*)-10-hydroxy-9-methoxy-11,13-dimethyloxacyclotetradeca-7,12-dien-2-one (9). Diene **13** (100 mg, 0.24 mmol) was dissolved in anhydrous degassed toluene (250 mL). The reaction was heated to reflux while stirring. The Grubbs-II generation catalyst (41 mg, 0.048 mmol) was dissolved in anhydrous degassed toluene (30 mL) and cannulated under positive nitrogen pressure to the reaction flask and the mixture was heated for 45 mins while heating at reflux. The solvent was then removed and flash chromatography (petroleum ether-EtOAc 100:1) gave a mixture of macrocyclic products (*Z:E*, 1:1, 44 mg, overall yield 46%). This mixture was dissolved in THF (3 mL) and transferred to a plastic vessel and then HF-pyridine (70%, 220 µL) was added dropwise and the resulting mixture was stirred for 24 h. The reaction was cooled to 0˚C and methoxytrimethylsilane (2.5 mL, 18 mmol) was added dropwise and the mixture stirred for 30 mins. The solvent was removed and chromatography of the residue (petroleum ether-EtOAc, 10:1) afforded **8** (16 mg, 21% from **13**) and **9** (16 mg, 21% from **13**). Analytical data for **8**: ^{1}H NMR (500 MHz, chloroform-d) δ 5.63 (ddd, *J* 15.6, 6.5, 5.2 Hz, 1H), 5.30-5.27 (dq, J 10.0, 2.0 Hz, 1H), 5.13 (ddt, *J* 15.6, 7.9, 1.7 Hz, 1H), 4.44 (dd, *J* 12.3, 1.1 Hz, 1H) & 4.36 (d, *J* 12.4 Hz, 1H), 3.40 (s, 1H, OH), 3.28 (t, *J* 8.8 Hz, 1H), 3.25 (s, 3H, OMe), 3.20 (t, *J* 8.2 Hz, 1H), 2.46-2.40 (m, 1H), 2.38 (overlapped signals, 2H), 2.20-2.11 (m, 1H), 2.05-1.96 (m, 1H), 1.80 – 1.73 (m, 1H), 1.73 – 1.66 (m, 1H), 1.65 (d, *J* 0.93 Hz, 3H, CH_3), 1.46 – 1.38 (overlapped signals, 2H), 1.08 (d, *J* 6.7 Hz, 3H, CH_3); ^{13}C NMR (126 MHz, chloroform-d) δ 173.5 (C), 134.9 (CH), 132.7 (CH), 128.2 (C), 126.4 (CH), 86.6 (CH), 77.6 (CH), 69.4 (CH_2), 55.8 (CH_3), 37.7 (CH), 34.1 (CH_2), 29.5 (CH_2), 26.1 (CH_2), 23.6 (CH_2), 18.6 (CH_3), 15.1 (CH_3); HRMS-ESI: Calcd for $C_{16}H_{26}O_4Na$: 305.1729; Found 305.1719 ($M+Na^+$). Analytical data for **9**: ^{1}H NMR (500 MHz, chloroform-d) δ 5.77 (m, 1H), 5.49 (apt t, *J* 10.5 Hz, 1H), 5.25 (d, *J* 10.2 Hz, 1H), 4.98 (dd, *J* 11.7 Hz, 1Hz, 1H), 4.12 (d, *J* 11.7 Hz, 1H), 3.91 (d, *J* 10.0 Hz, 1H), 3.25 (s, 3H, MeO), 2.98 (apt t, *J* 9.2 Hz, 1H), 2.69 (tq, *J* 9.9, 6.7 Hz, 1H), 2.40 (overlapped signals, 2H), 2.25 (d, *J* 9.6 Hz, 1H, OH), 2.18 (m, 1H), 1.89 – 1.81 (m, 1H), 1.80 (s, 3H), 1.79 – 1.72 (m, 1H, H-6b), 1.63 (m, 1H), 1.51 – 1.42 (m, 1H), 1.24 – 1.16 (m, 1H), 1.05 (d, *J* 6.7 Hz, 3H, CH_3); ^{13}C NMR (126 MHz, chloroform-d) δ 173.1 (CH), 133.8 (CH), 133.5 (CH), 132.1 (C), 128.4 (CH), 78.8 (CH), 74.3 (CH), 68.7 (CH_2), 55.7 (CH_3), 36.5 (CH), 32.8 (CH_2), 28.3 (CH_2), 27.1 (CH_2), 24.7 (CH_2), 17.3 (CH_3), 15.7 (CH_3). ESI/MS (*m/z*): 305.2 ($M+Na^+$); HRMS-ESI: Calcd for $C_{16}H_{26}O_4Na$ ($M+Na^+$): 305.1729; Found 305.1735.

(6*Z*,8*S*,9*S*,10*R*,11*E*)-9,13-Dihydroxy-8-methoxy-10,12-dimethyltrideca-6,11-dienoic acid (6). Compound **9** (3 mg, 0.011 mmol) was dissolved in (1:1 MeOH-H_2O) at room temperature. To it was added NaOH (180 µL, 0.09 mmol, 0.5 M). After stirring for 16 h, the mixture was concentrated and taken up in DCM. The mixture was acidified to pH 1 with 1 M HCl under stirring. The aq layer was separated and the organic layer was dried over Na_2SO_4 and concentrated to yield the furnished title compound (2.4 mg, 73%) as a clear oil; ^{1}H NMR (600 MHz, chloroform-d) δ 5.71 (dt, *J* 11.1, 7.4 Hz, 1H), 5.41 - 5.33 (overlapped signals), 4.04 (s, 2H), 3.91 (dd, *J* 9.7, 4.5 Hz, 1H), 3.25 (s, 3H, OMe), 3.22 (dd, *J* 6.5, 4.5 Hz, 1H), 2.65 (m, 1H), 2.35 (overlapped signals, 2H), 2.11 (overlapped signals, 2H), 1.70 - 1.64 (overlapped signals, 5H), 1.45 (overlapped signals, 2H), 1.00 (d, *J* 6.6 Hz, 3H); ^{13}C NMR (151 MHz, chloroform-d) δ 177.4 (C=O), 134.9 (CH), 134.5 (C), 128.8 (CH), 127.8 (CH), 78.1 (CH), 76.8 (CH), 68.6 (CH_2OH), 56.1 (OCH_3), 34.9 (CH), 33.7 (CH_2), 29.0 (CH_2), 27.6 (CH_2), 24.4 (CH_2), 16.0 (CH_3), 13.9 (CH_3); HRMS-ESI: calcd for $C_{16}H_{27}O_5$: 299.1858; Found 299.1854.

***N*-((4*R*,5*S*,6*S*,*E*)-5-(tert-Butyldimethylsilyloxy)-6-methoxy-2,4-dimethylocta-2,7-dienyl)hept-6-enamide (14).** To alcohol **12** (520 mg, 1.66 mmol) in anhydrous toluene (5 mL) was added diphenylphosphoryl azide (536 µL, 2.49 mmol) and DBU (372 µL, 2.49 mmol). The mixture was stirred for 5 h, then satd aq NH_4Cl solution was added and then Et_2O (30 mL). The organic layer was separated and the aq layer was extracted with Et_2O (3 x 20 mL). The combined organic layers were dried over Na_2SO_4 and the solvent was removed. Flash chromatography (petroleum ether-EtOAc 30:1) afforded a mixture of the azide intermediate (503 mg) as a

colourless oil (note that allylic azides can undergo 1,3-sigmatropic rearrangement and primary and allylic azides can be equilibrating). This mixture of allylic azides (503 mg, 1.48 mmol) was dissolved in THF (15 mL) and the contents were brought to heat at reflux and then triphenylphosphine (0.679 g, 2.59 mmol) and H_2O (133 µL, 7.4 mmol) were added. The mixture was heated and stirred at reflux for 6 h and the solvent was then removed. The residue was dissolved in anhydrous dichloromethane (10 mL) and DIPEA (1.03 mL, 5.92 mmol), EDC (567 µL, 2.96 mmol) and 6-heptenoic acid (401 µL, 2.96 mmol) were added. The mixture was stirred for 1 h and concentrated to a volume of ~2 mL. Flash chromatography (petroleum ether-EtOAc 6:1) afforded amide **14** (229 mg, 37% from **12**) as a clear oil: ^{1}H NMR (500 MHz, chloroform-d): δ 5.79 (m, 1H), 5.63 (m, 1H), 5.34 (br s, 1H, NH), 5.33 – 5.22 (overlapped signals, 3H), 5.03 – 4.92 (overlapped signals, 2H), 3.81 (dd, *J* 14.7, 6.0 Hz, 1H), 3.72 (dd, *J* 14.7, 5.5, 1H), 3.46 (dd, *J* 7.0, 3.2 Hz, 1H), 3.39 (t, *J* 7.5 Hz, 1H), 3.20 (s, 3H), 2.53 (m, 1H), 2.20 – 2.15 (overlapped signals, 2H), 2.10 – 2.03 (overlapped signals, 2H), 1.71 – 1.62 (overlapped signals, 2H), 1.57 (d, *J* 1.4 Hz, 3H), 1.42 (overlapped signals, 2H), 0.91 – 0.88 (overlapped signals, 12H), 0.06 (s, 3H), 0.01 (s, 3H); ^{13}C NMR (126 MHz, $CDCl_3$) δ 172.8 (C), 138.6 (CH), 135.3 (CH), 131.7 (CH), 130.3(C), 118.7 (CH_2), 114.8 (CH_2), 86.4 (CH), 78.1 (CH), 56.3 (CH_3), 47.0 (CH_2), 36.9 (CH_2), 34.5 (CH), 33.6 (CH_2), 28.7 (CH_2), 26.3 (CH_3), 25.4 (CH_2), 18.7 (C), 14.8 (CH_3), 14.1 (CH_3), -3.6 (CH_3), -4.6 (CH_3); HRMS-ESI: calcd for $C_{24}H_{45}NO_3SiNa$: 446.3066; Found 446.3066 ($M+Na^+$).

(7*Z*,9*S*,10*S*,11*R*,12*E*)-10-Hydroxy-9-methoxy-11,13-dimethylazacyclotetradeca-7,12-dien-2-one (10). The amide **14** (80 mg, 0.19 mmol) was dissolved up in anhydrous degassed toluene (250 mL) and the mixture heated to reflux while stirring. The Grubbs-II generation catalyst (34 mg, 0.038 mmol) was dissolved in anhydrous degassed toluene (30 mL) and added to the reaction flask via cannula and the mixture was then heated for 45 mins at reflux. The contents were concentrated under reduced pressure and flash chromatography (petroleum ether-EtOAc, 6:1) afforded the protected *cis* precursor (20 mg, 26%) as well as the *trans* precursor (16.5 mg, 22%). Analytical data for the *cis* intermediate ^{1}H NMR (500 MHz, chloroform-d) δ 5.85 (dd, *J* 7.2, 4.1 Hz, 1H, NH), 5.65 (td, *J* 10.4, 5.5 Hz, 1H), 5.26 (t, *J* 10.6 Hz, 1H), 5.08 (d, *J* 10.3 Hz, 1H), 4.20 (dd, *J* 16.2, 8.4 Hz, 1H), 3.83 (dd, *J* 10.2, 5.3 Hz, 1H), 3.44 – 3.35 (overlapped signals, 2H), 3.18 (s, 3H, OMe), 2.83 – 2.74 (m, 1H), 2.38 – 2.28 (overlapped signals, 2H), 2.22 (m, 1H), 2.00 (m, 1H), 1.84 (m, 1H), 1.67 (s, 3H, CH_3), 1.65 – 1.51 (overlapped signals, 2H), 1.35 (m, 1H), 0.94 (d, *J* 7.3 Hz, 3H, CH_3), 0.89 (overlapped singlets, 9H, 3 x CH_3), 0.06 (overlapped singlets, 6H, 2 x CH_3); ^{13}C NMR (126 MHz, $CDCl_3$) δ 172.0 (C), 133.3 (CH), 132.9 (C), 128.4 (CH), 125.8 (CH), 80.4 (CH), 78.0 (CH), 55.8 (CH_3), 44.8 (CH_2), 37.8 (CH), 35.2 (CH_2), 27.7 (CH_2), 27.1 (CH_2), 26.3 (CH_3), 24.6 (CH_2), 18.9 (CH_3) , 18.7 (C), 16.1 (CH_3), -3.8 (CH_3), -4.1 (CH_3). HRMS-ESI: Calcd for $C_{22}H_{41}NO_3SiNa$: 418.2753; Found 418.2754 ($M+Na^+$). Analytical data for the *trans* intermediate: ^{1}H NMR (500 MHz, chloroform-d) δ 5.67 (dt, *J* 14.1, 6.6 Hz, 1H), 5.47 (t, *J* 5.8 Hz, 1H, NH), 5.33 - 5.24 (overlapped signals, 2H, overlapping peaks), 3.83 (dd, *J* 15.3, 6.9 Hz, 1H), 3.62 (dd, *J* 15.6, 5.1 Hz, 1H), 3.56 (t, *J* 6.6 Hz, 1H), 3.36 - 3.31 (m, 1H), 3.21 (s, 3H, OMe), 2.55 - 2.47 (m, 1H), 2.33 - 2.20 (overlapped signals, 2H), 2.11 - 2.04 (overlapped signals, 2H), 1.77 - 1.68 (overlapped signals, 2H), 1.61 (d, *J* 1.2 Hz, 3H), 1.55 - 1.45 (overlapped signals, 2H), 0.97 (d, *J* 7.1 Hz, 3H, CH_3), 0.89 (9H, TBS group $C(CH_3)_3$), 0.08 (s, 3H, CH_3), 0.07 (s, 3H, CH_3); ^{13}C NMR (126 MHz, chloroform-d) δ 172.6 (C=O), 133.2 (CH), 131.1 (C), 128.5 (CH), 127.3 (CH), 87.9 (CH), 78.8 (CH), 56.2 (O*C*H_3), 45.8 (CH_2N), 38.4 (CH), 36.1 (CH_2), 30.6 (CH_2), 26.8 (CH_2), 26.2 (C(*C*H_3)$_3$), 24.2 (CH_2), 19.1 (CH_3), 18.5 (*C*(CH_3)$_3$), 16.1 (CH_3), -4.0 (Si*C*H_3), -4.5 (Si*C*H_3); IR (ATR) cm^{-1}: 3260, 2926, 1638, 1248, 832, 775; ESI/MS (*m/z*): ($M+Na^+$); 418.3 HRMS-ESI: Calcd for $C_{22}H_{41}NO_3SiNa$: 418.2753; Found 418.2752. The *cis* intermediate (16 mg, 0.041 mmol) was dissolved in THF (3 mL) and transferred to a plastic reaction vessel and HF-pyridine (70%, 10 mL) was added dropwise and the resulting mixture was stirred for a further 24 h. The reaction temperature was reduced to 0 ºC and methoxytrimethylsilane (2.5 mL, 18 mmol) was added dropwise to quench the reaction. This was stirred for a further 30 mins. The solvent was removed and chromatography of the residue (EtOAc

100%) gave **10** (10 mg, 90%); ^{1}H NMR (500 MHz, chloroform-d) δ 5.77 (br s, 1H, NH), 5.73 (td, *J* 10.4, 6.1 Hz, 1H), 5.39 (t, *J* 10.6 Hz, 1H), 5.09 (d, *J* 10.1 Hz, 1H), 4.07 (dd, *J* 15.9, 7.7 Hz, 1H), 3.93 (dd, *J* 10.0, 3.6 Hz, 1H), 3.54 (dd, *J* 16.0, 5.3 Hz, 1H), 3.24 (s, 3H, OMe), 3.16 (dd, *J* 7.4, 3.5 Hz, 1H), 2.72 (m, 1H), 2.47 (s, 1H, OH) 2.31 – 2.24 (overlapped signals), 1.95 (m, 1H), 1.83 (m, 1H), 1.72 (s, 3H, CH_3), 1.68 – 1.52 (overlapped signals, overlapping with signal for water also), 1.29 (m, 1H), 1.01 (d, *J* 7.0 Hz, 3H, CH_3); ^{13}C NMR (126 MHz, chloroform-d) δ 172.0 (C), 134.2 (CH), 133.7 (C), 128.0 (CH), 126.8 (CH), 79.3 (CH), 75.9 (CH), 55.8 (CH_3), 45.0 (CH_2), 36.3 (CH), 35.4 (CH_2), 28.1 (CH_2), 27.5 (CH_2), 24.6 (CH_2), 18.0 (CH_3), 16.1 (CH_3); HRMS-ESI: Calcd for $C_{16}H_{27}NO_3Na$: 304.1889; Found 304.1888 ($M+Na^+$)

(7*E*,9*S*,10*S*,11*R*,12*E*)-10-Hydroxy-9-methoxy-11,13-dimethylazacyclo-tetradeca-7,12-dien-2-one (7). The *trans* intermediate (16 mg, 0.041 mmol), obtained during preparation of **10**, was dissolved in THF (3 mL) and transferred to a nalgene falcon tube. HF in pyridine (70%, 220 µL) was added dropwise and the resulting mixture was stirred for 24 h at room temperature. The temperature was reduced to 0 °C via an ice bath and methoxytrimethylsilane (2.5 mL, 18.1 mmol) was added dropwise to quench the reaction. This was stirred for a further 30 min at room temperature. The mixture was concentrated and chromatography (EtOAc) afforded **7** (10 mg, 90%) as a white solid; ^{1}H NMR (500 MHz, chloroform-d) δ 5.63 (ddd, *J* 15.6, 7.5, 5.1 Hz, 1H), 5.46 (s, 1H, NH), 5.18 (dd, *J* 15.4, 7.6 Hz, 1H), 5.10 (d, *J* 9.6 Hz, 1H), 4.00 (dd, *J* 15.5, 7.7 Hz, 1H), 3.47 (dd, *J* 15.3, 4.4 Hz, 1H), 3.29 - 3.26 (m, 1H), 3.25 (s, 3H, OMe), 3.20 (t, *J* 7.9 Hz, 1H), 2.43 (m, 1H), 2.29 - 2.22 (overlapped signals, 2H), 2.21 - 2.15 (m, 1H), 2.07 - 1.95 (m, 1H), 1.80 - 1.73 (m, 1H), 1.69 - 1.64 (m, 1H), 1.63 (s, 3H), 1.60 - 1.47 (overlapped signals, 2H), 1.06 (d, *J* 6.7 Hz, 3H); ^{13}C NMR (126 MHz, chloroform-d) δ 172.8 (C=O), 134.3 (CH), 131.1 (C), 128.7 (CH), 126.7 (CH), 86.2 (CH), 78.4 (CH), 55.9 (O*C*H_3), 45.5 (CH_2N), 37.2 (CH), 36.2 (CH_2), 30.0 (CH_2), 26.2 (CH_2), 24.3 (CH_2), 18.8 (CH_3), 16.2 (CH_3); IR (ATR) cm^{-1}: 3323, 3194, 1641, 1557,1247, 962; HRMS-ESI: Calcd for $C_{16}H_{27}NO_3Na$: 304.1889; Found 304.1883 ($M+Na^+$)

Single crystal X-ray diffraction

An Oxford Diffraction Xcalibur system was used to collect X-ray diffraction data at ambient temperature for HPS. The crystal structure was solved by direct methods (ShelxT) and refined by full matrix least-squares using Shelxl-2014 within the Oscail package.[35-36] The crystal structure data has been deposited at the Cambridge Crystallographic Database (CCD). The deposition number is 1015786.

Molecular modeling

The coordinates for **10** (**SMGS4**) obtained from the X-ray crystal structure, provided the starting point for the conformational search The OPLSAA force field as implemented in Macromodel (www.schrodinger.com) was used. In total, for the conformational search, 10,000 conformers were generated using the MCMM method and each of these was minimised to convergence using the PRCG method. Each conformer generated was minimised in a solvent free environment and energies calculated. Conformers with energy values > 12 kJ/mol above the minimum were rejected during this analysis.

In vitro wound healing assays

The scratch assay was typically carried out to assess the influence of migrastatin analogues on cancer-cell motility. The cells were seeded at high density on FalconTM 6-well cell culture plates (Thermo Fisher Scientific, USA). After 24 h, when a 100% confluence was reached, the medium was removed and replaced with medium containing one of the migrastatin analogues or DMSO (control) at a concentration of 10µM. The monolayer was wounded by scratching the surface as uniformly and straight as possible with a pipette tip (1000 µL) at least four times. Images of cells invading the scratch were captured at indicated time points (0, 6, 12 and 24 h) by using a phase-contrast Olympus CKX41SF microscope (Olympus Corporation, Japan). The pictures were analyzed with ImageJ 1.50b (National Institutes of Health, USA). The migration rate was expressed as percentage of scratch closure and was calculated as follows: percentage of scratch closure = 100*(a – b)/a,

where a is the surface area at time point 0 h, and b is the surface area that remained cell-free after 24 h of migration. The values are represented as means of three different wound fields from three independent experiments (n = 9).

Statistical analysis

Statistical analysis was carried out by using GraphPad Prism 7.0 software (GraphPad Software, USA). The in-vitro wound-healing assay and transwell migration assay were analyzed by using the one-way ANOVA, the Dunnett's post-hoc test and the t-test. A p-value of <0.05 was regarded as significant, whereas p-values of <0.01 and <0.001 were regarded as highly significant. The data is expressed as mean ± standard deviation.

Supplementary material

NMR spectra of **6-10.**

Acknowledgements

This research was supported by Science Foundation Ireland (Grant Nos. 07/IN.1/B966 and 11/TIDA/B2047) and by the Irish Research Council (PhD scholarship to SS). PVM and SS thank Sinbad Sweeney and Prof. Teresa Tetley (Lung Cell Biology, NHLI, Imperial College London, London SW3 6LY) for performing A549 cell migration and wound closures assays.

References

1. Nakae, N.; Yoshimoto, Y.; Ueda, M.; Sawa, T.; Takahashi, Y.; Naganawa, H.; Takeuchi, T.; Imoto, M. J. *J. Antibiot.* **2000**, *53*, 1228-30. https://doi.org/10.7164/antibiotics.53.1228
2. Woo, E. J.; Starks, C. M.; Carney, J. R.; Arslanian, R.; Cadapan, L.; Zavala, S.; Licari, P. *J. Antibiot.* **2002**, *55*, 141-6. https://doi.org/10.7164/antibiotics.55.141
3. Ju, J.; Lim, S.-K; Jiang, H.; Shen, B. *J. Am. Chem. Soc.* **2005**, *127*, 1622-1623. https://doi.org/10.1021/ja043808i
4. Wach, J.-Y.; Gademann, K. *Synlett* **2012**, 23, 163-170. https://doi.org/10.1055/s-0031-1290125
5. Gaul, C.; Njardarson, J. T.; Shan, D.; Dorn, D. C.; Wu, K.-D.; Tong, W.P.; Huang, X.-Y.; Moore, M. A. S. Danishefsky, S. J. *J. Am. Chem. Soc.* **2004**, *126*, 11326-37. https://doi.org/10.1021/ja048779q
6. Shan, D.; Chen, L.; Njardarson, J. T.; Gaul, C.; Ma, X.; Danishefsky, S. J.; Huang, X.-Z. *Proc. Nat. Acad. Sci. USA* **2005**, *102*, 3772–76. https://doi.org/10.1073/pnas.0500658102
7. Oskarsson, T.; Nagorny, P.; Krauss, I. J.; Perez, L.; Mandal, M.; Yang, G.; Ouerfelli, O.; Xiao, D.; Moore, M. A. S.; Massagu, M.; Danishefsky, S. J. *J. Am. Chem. Soc.*, **2010**, *132*, 3224-28. https://doi.org/10.1021/ja9101503

8. Majchrzak, K.; Lo Re, D.; Gajewska, M.; Bulkowska, M.; Homa, A.; Pawłowski, K.; Motyl, T.; Murphy, P. V.; Król, M. *PlosOne*, **2013**, *8*, e76789 https://doi.org/10.1371/journal.pone.0076789
9. Lo Re, D.; Zhou, Y.; Nobis, M.; Anderson, K. I.; Murphy, P. V. *ChemBioChem*, **2014**, *15*, 1459–64. https://doi.org/10.1002/cbic.201402061
10. Reymond, S.; Cossy, J. *Comptes Rendus Chimie* **2008**, *11*, 1447-62. https://doi.org/10.1016/j.crci.2008.08.004
11. Oskarsson, T. ; Nagorny, P.; Krauss, I. J.; Perez, L.; Mandal, M.; Yang, G.; Ouerfelli, O.; Xiao, D.; Moore, M. A. S.; Massague, J.; Danishefsky, S. J. *J. Am. Chem. Soc.* **2010**, *132*, 3224-28. https://doi.org/10.1021/ja9101503
12. Gade, N. R.; Iqbal, J. *Tetrahedron Lett.* **2013**, *54*, 4225-27. https://doi.org/10.1016/j.tetlet.2013.05.137
13. Rajski, S. R.; Shen, B. *ChemBioChem* **2010**, *11*, 1951-54. https://doi.org/10.1002/cbic.201000370
14. Ju, J.; Rajski, S. R.; Lim, S.-K.; Seo, J.-W.; Peters, N. R.; Hoffmann, F.; Shen, B. *J. Am. Chem. Soc.* **2009**, *131*, 1370-71. https://doi.org/10.1021/ja808462p
15. Lecomte, N.; Njardarson, J. T.; Nagorny, P.; Yang, G.; Downey, R.; Ouerfelli, O.; Moore, M. A.; Danishefsky S. J. *Proc Natl Acad Sci USA* **2011**, *108*, 15074-78. https://doi.org/10.1073/pnas.1015247108
16. Dias, L. C. ; Finelli, F. G.; Conegero, L. S.; Krogh, R.; Andricopulo, A. D. *Eur. J. Org. Chem*, **2010**, 6748-6759. https://doi.org/10.1002/ejoc.201001097
17. Anquetin, G.; Rawe, S. L.; McMahon, K.; Murphy E.; Murphy, P. V. *Chem. Eur. J.* **2008**, *14*, 1592–600. https://doi.org/10.1002/chem.200701033
18. Anquetin, G.; Horgan, G.; Rawe, S.; Murray, D.; Madden, A.; MacMathuna, P.; Doran P.; Murphy, P. V. *Eur. J. Org. Chem.* **2008**, *11,* 1953-8. https://doi.org/10.1002/ejoc.200701192
19. Zhou, Y.; Murphy, P. V. *Tetrahedron Lett.* **2010**, *51*, 5262-5264. https://doi.org/10.1016/j.tetlet.2010.07.141
20. Francis, F.; Croft, D.; Schüttelkopf, A. W.; Parry, C.; Pugliese, A.; Cameron, K.; Claydon, S.; Drysdale, M.; Gardner, C.; Gohlke, A.; Goodwin, G.; Gray, C. H.; Konczal, J.; McDonald, L.; Mezna, M.; Pannifer, A.; Paul, N. R.; Machesky, L.; McKinnon, H.; Bower, J. *Bioorg. Med. Chem. Lett.* **2019**, *29*, 1023-29. https://doi.org/10.1016/j.bmcl.2019.01.035
21. Grubbs, R. H. *Tetrahedron* **2004**, *60*, 7117-40. https://doi.org/10.1016/j.tet.2004.05.124
22. Lo Re, D.; Zhou, Y.; Mucha, J.; Leahy, L. C.; Jones, L. F.; Santocanale, C.; Król, M.; Murphy, P. V. *Chem. Eur. J.* **2015**, *21*, 18109–121. https://doi.org/10.1002/chem.201502861
23. Navarro-Vazquez, A.; Cobas, J. C.; Sardina, F. J.; Casanueva, J.; Daez, E. *J. Chem. Inform. Comp. Sci.* **2004**, *44*, 1680-85. https://doi.org/10.1021/ci049913t
24. Karplus, M. *J. Phys. Chem.* **1959**, *30*, 11. https://doi.org/10.1063/1.1729860
25. Karplus, M. *J. Am. Chem. Soc.* **1963**, *85*, 2870-71.

https://doi.org/10.1021/ja00901a059
26. Barfield, M.; Smith, W. B. *J. Am. Chem. Soc.* **1992**, *114*, 1574. https://doi.org/10.1021/ja00031a006
27. Smith, W. B.; Barfield, M. *Magn. Reson. Chem.* **1993**, *31*, 696. https://doi.org/10.1002/mrc.1260310719
28. Mohamadi, F.; Richards, N. G. J.; Guida, W. C.; Liskamp, R.; Lipton, M.; Caufield, C.; Chang, G.; Hendrickson, T.; Still, W. C. *J. Comput. Chem.* **1990**, *11*, 440. https://doi.org/10.1002/jcc.540110405
29. Jorgensen, W. L.; Maxwell, D. S.; Tirado-Rives, J. *J. Am. Chem. Soc.* **1996**, *118*, 11225. https://doi.org/10.1021/ja9621760
30. Bradley, H.; Fitzpatrick, G.; Glass, W. K.; Kunz, H.; Murphy, P. V. *Org. Lett.* **2001**, *3*, 2629-32. https://doi.org/10.1021/ol016294q
31. Murphy, P. V.; Bradley, H.; Tosin, M.; Pitt, N.; Fitzpatrick, G. M.; Glass, W. K. *J. Org. Chem.* **2003***, 68*, 5693-5704. https://doi.org/10.1021/jo034336d
32. Velasco-Torrijos, T.; Murphy, P. V. *Tetrahedron Asymm.* **2005**, *16*, 261-272. https://doi.org/10.1016/j.tetasy.2004.11.020
33. André, S.; Wang, G.-N.; Gabius H.-J.; Murphy, P. V. *Carbohydr. Res.* **2014**, *389*, 25–38. https://doi.org/10.1016/j.carres.2013.12.024
34. Doyle, D.; Murphy, P. V. *Carbohydr. Res.* **2008**, *343*, 2535-44. https://doi.org/10.1016/j.carres.2008.06.007
35. Sheldrick, G. *Acta Crystallographica Section A*, **2008**, *64*, 112-122. https://doi.org/10.1107/S0108767307043930
36. McArdle, P.; Hu, Y.; Lyons, A.; Dark, R. *Crystengcomm* **2010**, *12*, 3119-25. https://doi.org/10.1039/c001071e